Shape and Form Optimization of On-Line Pressure-Compensating Drip Emitters to Achieve Lower Activation Pressure

Citation: Shamshery, Pulkit, and Amos G. Winter. "Shape and Form Optimization of On-Line Pressure-Compensating Drip Emitters to Achieve Lower Activation Pressure." Journal of Mechanical Design 140, 3 (December 2017): 035001 © 2018 ASME

As Published: http://dx.doi.org/10.1115/1.4038211

Publisher: ASME International

Persistent URL: http://hdl.handle.net/1721.1/120089

Version: Final published version: final published article, as it appeared in a journal, conference proceedings, or other formally published context

Shape and Form Optimization of On-Line Pressure-Compensating Drip Emitters to Achieve Lower Activation Pressure

Pulkit Shamshery
Global Engineering and Research Laboratory,
Massachusetts Institute of Technology,
Cambridge, MA 02139
e-mail: ps544@mit.edu

Amos G. Winter V[1]
Mechanical Engineering Global Engineering and Research Laboratory,
Massachusetts Institute of Technology,
Cambridge, MA 02139
e-mail: awinter@mit.edu

This study presents the design and validation of on-line pressure-compensating (PC) drip irrigation emitters with a substantially lower minimum compensating inlet pressure (MCIP) than commercially available products. A reduced MCIP, or activation pressure, results in a drip irrigation system that can operate at a reduced pumping pressure, has lower power and energy requirements, requires a lower initial capital cost, and facilitates solar-powered irrigation systems. The technology presented herein can help spread drip irrigation to remote regions and contribute to reducing poverty, particularly in developing countries. The activation pressures of drip emitters at three flow rates were minimized using a genetic algorithm (GA)-based optimization method coupled with a recently published fluid–structure interaction analytical model of on-line PC drip emitter performance. The optimization took into account manufacturing constraints and the need to economically retrofit existing machines to manufacture new emitters. Optimized PC drip emitter designs with flow rates of 3.3, 4.2, and 8.2 lph were validated using precision machined prototype emitters. The activation pressure for all was ≤0.2 bar, which is as low as 16.7% that of commercial products. A limited production run of injection molded 8.2 lph dripper prototypes demonstrated they could be made with conventional manufacturing techniques. These drippers had an activation pressure of 0.15 bar. A cost analysis showed that low MCIP drip emitters can reduce the cost of solar-powered drip irrigation systems by up to 40%.
[DOI: 10.1115/1.4038211]

1 Introduction

The objective of this study was to design and validate a suite of on-line pressure-compensating (PC) drip irrigation emitters with a substantially lower minimum compensating inlet pressure (MCIP) than commercially available drip emitters. PC drip irrigation systems use a unique drip emitter design to maintain a constant flow rate above the MCIP across a wide range of inlet pressures. PC behavior is advantageous because it results in a uniform distribution of water throughout a field, which helps maintain the optimal moisture content in the soil for all crops and ensure minimal water losses. While non-PC emitters are less expensive and can deliver relatively uniform flow for small fields, irrigation of larger fields (our target is ≥1 acre), which contain longer pipes with greater pressure drop, requires pressure compensation. Reducing the MCIP of drip emitters lowers the required pumping pressure, power, and capital cost of a drip irrigation system, which will make the technology more accessible to farmers throughout the world, particularly in developing countries.

Drip irrigation, compared to rainfed and flood irrigation, has been shown to increase yields for some crops by 20–90% while reducing water consumption by 30–70% across several regions in South Asia and East Africa [1–3]. Drip systems achieve this by applying water directly to the plant root system at a controlled flow rate through a series of drip emitters. Drip irrigation has also been shown to reduce fertilizer usage by up to 40%, to enable the growth of water-sensitive cash crops in areas where these crops would not normally be viable [1–4], and to produce labor savings due to reduced intercultivation tasks and automation capability [5,6]. Irrigation is one of the most effective means of lifting poor, subsistence farmers out of poverty by enabling them to grow more and higher-value crops [7–10].

In spite of these benefits, there are several constraints to the widespread adoption of drip irrigation. One major barrier is the high initial capital and operating cost of the drip system, particularly in off-grid or limited grid settings where most small and marginal farmers live [7–11]. One of the largest drivers of capital cost in a drip system (and recurring cost in diesel-powered systems) is the pumping cost. Pumping is required to overcome pressure losses in the filters, fittings, and piping (typically <0.6 bar [12–14]), to overcome the MCIP of PC drip emitters (typically ∼0.8–1 bar), and to pump water from the water source to the drip system. If surface water is assumed as the water source (water depth < 5 m, which is true for 63% of irrigated farms globally [15]), then the typical operating pumping pressure of the entire PC drip system is ∼2 bar [12–14], over 50% of which is used to overcome the MCIP. Reducing the MCIP can therefore be a highly effective way to reduce required pumping pressure, which will lower power and energy requirements and lower the initial capital cost of drip irrigation systems, reducing a major barrier to global dissemination. A drip irrigation system requiring less pumping pressure is also more amenable to fully off-grid pump systems, which can help spread drip irrigation to remote regions and contribute to reducing poverty.

Pressure-compensating behavior is achieved through the complicated fluid–structure interaction between a thin membrane and the flow channels within an emitter. Dripper architectures fall into two general categories: on-line emitters, which are typically installed on the outside of a pipe and can be placed to accommodate unevenly spaced crops; and in-line emitters, which are embedded directly into a pipe at fixed distances, allowing for rapid installation. The behavior of PC on-line drip emitters was recently analytically described using an iterative coupled fluid–structure interaction model, which took into account the membrane deflection and its interaction with the geometric flow path features within the dripper [16]. The development and validation of this model created a tool capable of optimizing the geometry and design of an on-line PC drip emitter to minimize MCIP.

The present study combines the coupled fluid–structure interaction model of on-line PC drip emitters with a genetic algorithm (GA) to optimize drippers' internal flow path geometry for minimized MCIP while maintaining constant flow rate across an expected operating pressure range. Insights from Jain Irrigation, a major global manufacturer and distributer of PC drip emitters based in Jalgaon, India, were used to add unique manufacturing constraints to the optimization. These constraints include conceivable dimensions of injection molded features and the need to economically retrofit existing injection-molding machines, ensuring that the new designs can be readily incorporated into existing manufacturing and distribution channels. The MCIP for an 8.2 lph dripper was minimized to 0.15 bar, which is compared to published MCIP values of off-the-shelf products from three major manufacturers: Jain Irrigation, Netafim, and Toro. Our dripper was found to have an MCIP as low as 16.7% that of the competing

[1]Corresponding author.
Contributed by the Design Engineering Division of ASME for publication in the Journal of Mechanical Design. Manuscript received June 5, 2017; final manuscript received October 3, 2017; published online December 21, 2017. Assoc. Editor: Yu-Tai Lee.

products. The reduced MCIP was validated using precision-machined prototype emitters and a limited run of injection-molded prototypes manufactured using retrofitted molds at Jain Irrigation, demonstrating that the new designs could be made with existing manufacturing equipment. Our optimization method was additionally tested at other flow rates by minimizing the MCIP for 3.3 and 4.2 lph drip emitters to $\leq$0.2 bar and validating their performance using precision-machined prototypes. This paper also presents a detailed analysis of the capital cost of fully off-grid, solar-powered drip irrigation systems to assess the competitive advantage low MCIP drip systems would have over currently available technology in off-grid markets. Component price lists relevant to global markets and specific to India were used to confirm that minimizing the MCIP of drip emitters could reduce the capital cost of off-grid systems by 27% in global markets and 40% in India specifically.

2 Coupled Fluid–Structure Interaction Model Used for Optimization

In prior work, the authors described a coupled fluid–structure interaction model to predict the volumetric flow rate as a function of inlet pressure in on-line PC drip emitters [16]. A summary of this model is provided in the following paragraphs. The qualitative working principle of a PC drip emitter is shown schematically in Fig. 1. Fluid flows into the emitter through the inlet at inlet pressure P_{inlet}. The fluid then flows from the top of the membrane into the chamber under the membrane through an orifice, which is the small gap between the self-sealing membrane and the surrounding structure (Fig. 1(*b*)). The flow through the orifice leads to a pressure loss and sets up the pressure loading on the membrane P_{loading}. The fluid then flows out of the emitter to the atmosphere at atmospheric pressure.

As P_{inlet} increases, the compliant membrane deflects down until it touches the lands (Fig. 1(*d*)). At this point, the fluid has to flow around the chamber and through the channel in the lands. As the inlet pressure increases further, the additional loading results in the membrane shearing into the channel (Fig. 1(*e*)). This reduces the cross-sectional area of the channel and increases flow resistance. The two primary resistances to fluid flow are shown in Figs. 1(*d*) and 1(*e*), with κ_o characterizing the fixed loss coefficient of the orifice, and κ_c characterizing the variable resistance of the channel that increases with pressure.

In the coupled fluid–structure interaction model, bending of the compliant membrane was characterized using Kirchhoff Love plate theory and then superimposing a large deflection correction

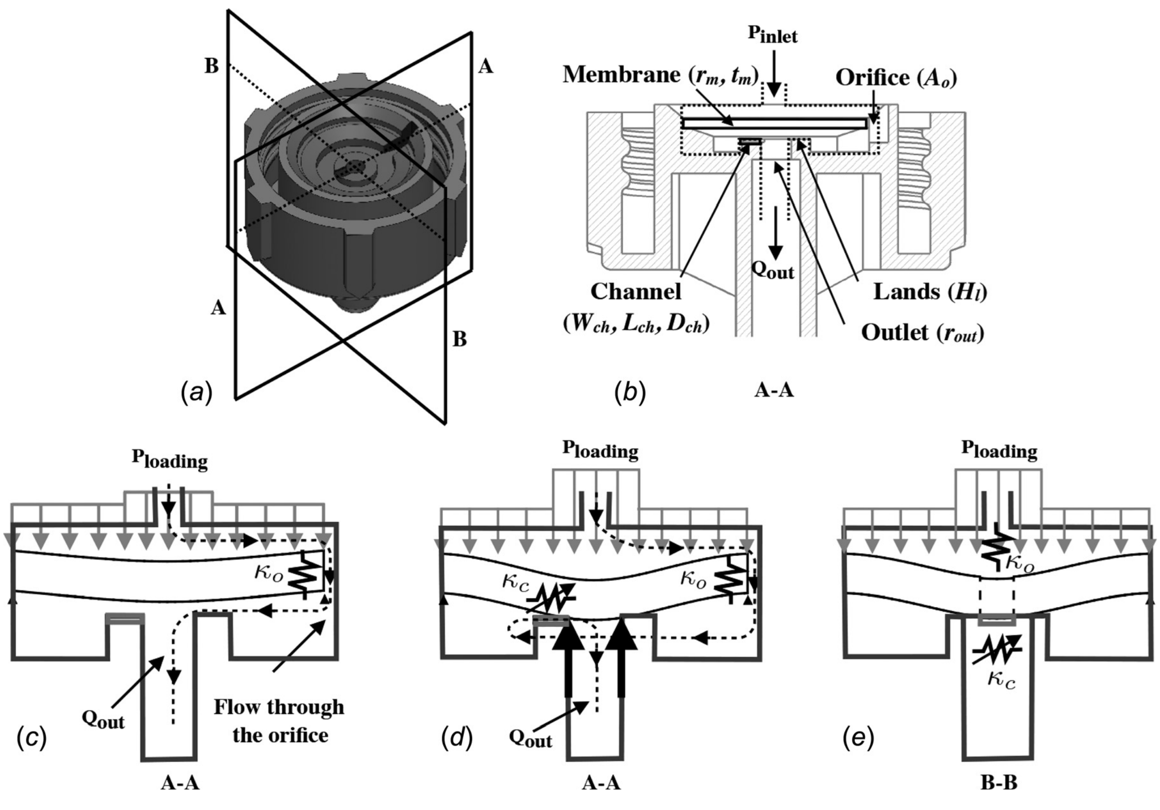

Fig. 1 Schematic of a conventional PC on-line emitter. (*a*) Isometric view of a characteristic, commercial online PC drip emitter. (*b*) View along the A-A plane pointing out the main topological features and listing the design variables taken into account in the coupled fluid–structure interaction analytical model (described in the text). (*c*) View along the A-A plane showing the flow path of water in the emitter for low inlet pressures. When the inlet pressure is low, the fluid flow path is not constrained and water can flow into the inlet, through the orifice, over the lands, and out the outlet. The fluid flow path is denoted by the dashed line with triangular arrow heads, driven by an input pressure of P_{inlet}. The main resistance to fluid flow is through the orifice, characterized by a loss coefficient κ_o. The flow of fluid through the emitter sets up a pressure differential across the membrane, as seen by the gray vertical arrows pointing at the membrane, P_{loading}. (*d*) View along the A-A plane showing the flow path of water in the emitter for high inlet pressures. As the inlet pressure increases, the compliant membrane deflects down to the lands resulting in an upward force being exerted on the membrane by the lands, shown by the large black arrows. Once the membrane contacts the lands, the fluid flow has to divert around the lands and flow through the channel and out through the outlet. The main resistances to fluid flow are now both the orifice and the channel, characterized by a loss coefficient κ_c. (*e*) View along the B-B plane showing the shearing of the membrane into the channel (vertical dashed lines on the membrane) as P_{inlet} increases from state d, which decreases the effective channel area and increases κ_c.

factor. The plate shearing into the channel was modeled by the shearing of a thick beam, as the ratio of length to width of the section of the membrane pushed into the channel is always greater than 5:1 for the relevant operating pressure range of drip emitters. Due to the steady nature of the membrane deformation and the fluid flow through the drip emitter, the coupled fluid–structure interaction mechanics was characterized using a segregated modeling technique. Here, the structural and fluid domains were solved separately and then coupled at their boundary. The structure deformation defined the flow path and the fluid pressure losses dictated the pressure differential acting on the membrane, causing its deformation. A full analytical and parametric description of the coupled fluid–structure interaction mechanics for how the membrane restricts water flow in the dripper can be found in Ref. [16].

Our coupled fluid–structure interaction model of on-line PC drip emitters is capable of taking the following geometric design variables as inputs (Fig. 1(*b*)):

x_1: membrane radius (r_m)
x_2: membrane thickness (t_m)
x_3: channel width (W_{ch})
x_4: channel length (L_{ch})
x_5: channel depth (D_{ch})
x_6: land to membrane clearance height (H_l)
x_7: orifice size (A_o)
x_8: outlet radius (r_{out})

The model uses these variables in an iterative fluid–structure interaction solver to calculate the flow rate out of the emitter for a given inlet pressure.

The robustness of this analytical model was validated using a commercially available 8 lph on-line drip emitter and eight prototypes that were derivatives of its design (each differing from the commercial emitter along one of the eight parameters x_1–x_8) [16]. In each case, the model predicted a flow rate as a function of pressure consistent with the measured values (to within $R^2 > 0.85$). Key insights from this work were that increasing channel depth (D_{ch}), decreasing channel width (W), decreasing effective channel length ($L_{ch,eff}$), and increasing the maximum height of deflection of the membrane (H_l) all lead to a measurable increase in flow rate for a given inlet pressure. The effective channel length $L_{ch,eff}$ is the length of the channel sealed by the membrane, which increases with pressure. It was noted that an increase in orifice size (A_o) led to a reduction in orifice losses (described by κ_o), which is critical to reducing the MCIP. The development and validation of this model created a tool capable of optimizing the geometry of PC on-line drip emitters to minimize orifice and channel losses, and thus minimize the MCIP.

3 Optimization of On-Line Pressure-Compensating Drip Emitter Architecture

The objective of this study was to use the coupled fluid–structure interaction model to optimize the geometry of an on-line PC drip emitter for lower MCIP compared to that of commercially available emitters. An ideal emitter would maintain a constant specified flow rate over the entire inlet pressure range, and have an activation pressure of 0 bar. The optimization problem aimed to determine the set of design inputs that minimized the deviation between the predicted flow rate of the designed emitter and the ideal constant flow rate (Eq. (1)). The objective function minimized the Euclidean distance between the predicted flow rate as a function of inlet pressure for the designed emitter and the ideal performance

$$J_1 = \min\left(\sum_{i=1}^{n} \|q_i^{\text{ideal}} - q_i^{\text{design}}\|\right) \quad (1)$$

Here n is the total discretization of inlet pressure, which was taken in this study to range from 0 to 1.5 bar in $n = 100$ equal units; q_i^{ideal} is the ideal flow rate at ith pressure discretization, which is a constant at the nominal rated flow rate; and q_i^{design} is the design flow rate at ith pressure discretization, which is the output from the coupled fluid–structure interaction model for the specified geometric design variables within the emitter.

The following series of constraints were enforced to represent realistic manufacturing and procurement constraints based on input from Jain Irrigation [17]. They result from the requirement of using existing injection molding machines to produce the new designs, which can be cost-effectively retrofitted with mold inserts for new emitter geometry. Furthermore, the dimensions of existing high-precision silicone membranes were retained, given that these are sourced from an outside manufacturer

g_1: $r_m = 5.5$ mm
g_2: $t_m = 1.2$ mm
g_3: $0.5\text{ mm} \le W_{ch} \le 2\text{ mm}$
g_4: $0.5\text{ mm} \le L_{ch} \le 2\text{ mm}$
g_5: $0.05\text{ mm} \le D_{ch} \le 1\text{ mm}$
g_6: $0 \le H_l \le 1\text{ mm}$
g_7: $0.5\text{ mm}^2 \le A_o \le 2\text{ mm}^2$
g_8: $0.05\text{ mm} \le r_{out} \le 2\text{ mm}$

The following parameters enforced on the membrane material (p) were based on measurements of membranes in commercially available 8 lph on-line drip emitters produced by Jain Irrigation [18].

p_1: Young's modulus (E) = 0.038 GPa
p_2: Shear modulus (G) = 0.6 MPa
p_3: Poisson's ratio (ν) = 0.48
p_4: membrane material = silicone

A genetic algorithm-based heuristic optimization method was used to find the global minimum of the objective function (Eq. (1)), while obeying the dimensional constraints. A GA-based approach was preferred over other optimization techniques because the objective function is a discontinuous function and the constraints are nonlinear; hence, the problem is amenable to a heuristic optimizer. Additionally, GAs are well suited for handling integer constraints, which are necessary to take into account the dimensional tolerances considered for injection molding. The GA optimization toolbox in MATLAB (The MathWorks, Natick, MA) was used. The following values for population size, mutation rate, and crossover rate were used to conduct the optimization study

Population size = 500 genes
Mutation rate = 0.03
Crossover rate = 0.8
Maximum generation = 20

Stopping conditions were set as follows: The deviation between ideal versus design flow rate is less than 5% OR the algorithm runs for 20 generations.

The iterative fluid–structure interaction model combined with the GA algorithm is shown schematically in Fig. 2. This procedure was followed to optimize the internal geometry of three emitters with objective flow rates (q^{ideal}) of 8, 6, and 5 lph, which were chosen to match commercially available emitter flow rates. The values for each geometric variable produced by the optimization are listed in Table 1. Each emitter had an orifice with a rectangular cross section of area $A_o = L_o W_o$.

4 Prototype Drip Emitter Design, Fabrication, Testing, and Error Analysis

For each target flow rate of 8 lph, 6 lph, and 5 lph, two prototype drip emitters with optimized geometric values given in Table 1 were precision machined from polyoxymethylene (delrin) using a milling machine. The combined machine resolution and tool offset of the computer numerical control mill was 0.01 mm. Target dimensions were validated using optical metrology (InfiniteFocus

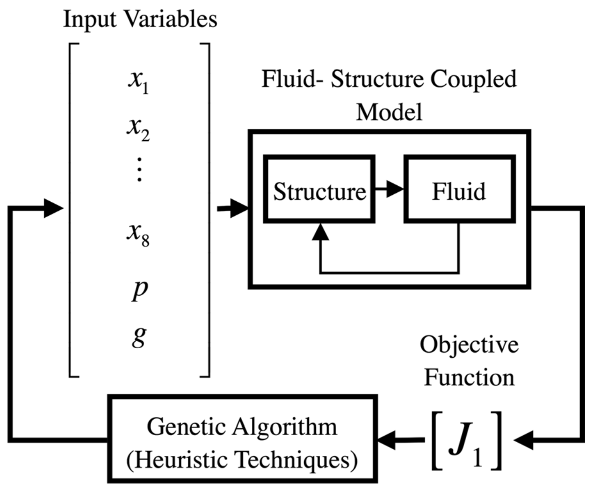

Fig. 2 Optimization method. Design variables (x_1–x_8), constraints (g_1–g_8) and parameters (p_1–p_4) are input into the analytical coupled fluid–structure interaction model presented in Ref. [16]. The model iterates between the individual structure and fluid analytical expressions until they converge, yielding a prediction of the flow rate versus pressure behavior of the dripper. This result is then evaluated with the objective function in Eq. (1). A GA is used to vary and test multiple sets of design variables to minimize the objective function.

Table 1 GA optimization results for geometric values corresponding to emitters with target flow rates of 8 lph, 6 lph, and 5 lph, and measured flow rates of 8.2 lph, 4.2 lph, and 3.3 lph, respectively

Variable (mm)	8 lph	6 lph	5 lph
r_m	5.50	5.50	5.50
t_m	1.20	1.20	1.20
W_{ch}	1.18	1.18	1.18
L_{ch}	1.40	1.40	1.40
D_{ch}	0.20	0.15	0.13
H_l	0.70	0.30	0.30
L_o	1.25	1.25	1.25
W_o	1.00	1.00	1.00
r_{out}	0.64	0.60	0.60
Measured flow rate (lph)	8.2	4.2	3.3

measurement machine, Alicona Imaging GmbH, Graz, Austria) and the largest variation detected was 0.07 mm.

To validate the flow rate as a function of inlet pressure in the prototype drip emitters, the standard procedure used to characterize commercial drip emitters as described in the ITRC technical report 2013 [19] was used. The prototypes were tested with this procedure to allow for comparisons to the published performance curves (e.g., flow rate as a function of inlet pressure) available for commercial drip emitters. The apparatus was comprised of a water supply capable of producing a constant inlet pressure (fully described later) attached to a length of hose (length 3 ft, diameter 0.5 in), which was held horizontally with the target drip emitters inserted no less than 12 in apart. The hose could be moved horizontally along a track, placing each drip emitter above its own 250 mL graduated cylinder at a designated time. A stop watch was used to measure the time required for the drip emitter to fill the entire 250 mL volume, and the average flow rate of the emitter was calculated to within ±5%. For each emitter, the average flow rate was measured eight times and the results averaged (standard deviation < 10%).

The apparatus to produce a water supply at constant inlet pressure was an air-pressurized tank of tap water connected to a pressure regulating valve. The inlet pressure was monitored by a Dwyer DPGW-07 (Dwyer Instruments, Inc., Michigan City, IN) pressure gauge. Before each flow rate measurement, the flow rate was allowed to equilibrate (discarding the output water) for 5 min pressurized at 1 bar, and then for 1 min at each imposed inlet pressure. The average flow rate of each emitter was measured in 0.1 bar increments for target inlet pressures of 0.1±0.05 bar to 1.6±0.05 bar. Throughout the experiments, the target pressure was stable to within ±0.02 bar.

The measured average flow rates as a function of inlet pressure for the machined prototype emitters based on the three optimized dripper geometries are presented in Fig. 3. Although the emitters were intended to produce 8 lph, 6 lph, and 5 lph, they were experimentally found to emit 8.2 lph, 4.2 lph, and 3.3 lph, respectively. Industry standards require the flow rate above the activation pressure to be within ±10% of the target flow rate. In each prototype case, the measured flow rates fall within these bounds for inlet pressures above 0.2±0.05 bar, indicating that the activation pressure is at or below this value. These results demonstrate that the optimized dripper geometries did produce three distinctly different flow rates at significantly lower MCIPs than commonly available commercial products. For each case, the theoretically predicted MCIP was very close to the experimentally measured value. Although there are significant deviations between the theoretical and experimental flow rate results, these three devices represent design innovations (which could translate into commercial products) for novel dripper architectures that should be rated at 8.2 lph, 4.2 lph, and 3.3 lph.

There are most likely multiple sources of error, which contributed to the inaccurate theoretical predictions shown in Fig. 3. The theory used in this study relies on an orifice loss coefficient (κ_o) that was experimentally measured to be 0.95 using commercial 8 lph emitters produced by Jain Irrigation [16]. In this prior work, it was found that increasing orifice cross-sectional area has a large effect on reducing the activation pressure; as such, the three prototypes designed and tested in this study had larger orifices than Jain's 8 lph dripper. Furthermore, the orifices had radiused corners from the milling process. To improve the theoretical model presented in Ref. [16], κ_o as a function of orifice size and shape should be experientially determined. The GA objective and nominal flow rate for the 8 lph dripper (Fig. 3(*a*)) are in closest agreement out of the three prototypes, which may be a result of the theory being based on Jain's 8 lph emitter.

Manufacturing errors may have also played a role in the theoretical versus experimental discrepancy. Our prior publication on drip emitter theory [16] did not consider how geometric tolerances could affect the pressure–flow rate relationship. Figure 4 is a modified reproduction of results from Ref. [16] showing the variation of anticipated flow rate for Jain's 8 lph emitter over the same pressure range investigated in this study. The modeled manufacturing tolerances are ±0.01 mm on D_{ch} and ±0.05 mm on W_{ch}, which are within the expected manufacturing and shrinkage variations that could be expected for a polypropylene injection molded part the size of the dripper [20,21]. The 6 lph and 5 lph optimized drippers have shallower channels than the optimized 8 lph and Jain's 8 lph ($D_{ch} = 0.3$ mm) emitters. This would make the lower flow rate drippers more sensitive to manufacturing tolerances and could have contributed to the greater error in the theory.

Since the design and optimization method presented in this paper did successfully produce three distinct, low-MCIP emitter architectures, these results can be used to form a correction factor for the fluid-structure interaction model presented in Ref. [16]. Using the data in Table 1, the nominal ideal flow rates that are predicted by the theoretical model (q^{ideal}) using the optimized geometry can be correlated to the expected measured flow rates (q^{measured}) with

$$q^{\text{measured}} = 0.134(q^{\text{ideal}})^2 - 0.056q^{\text{ideal}} \qquad (2)$$

Equation (2) has an intercept of 0, 0 (forcing it to realistic behavior at zero pressure) and $R^2 = 0.99$ using the data from Table 1. Although the fluid–structure interaction theory from Ref. [16]

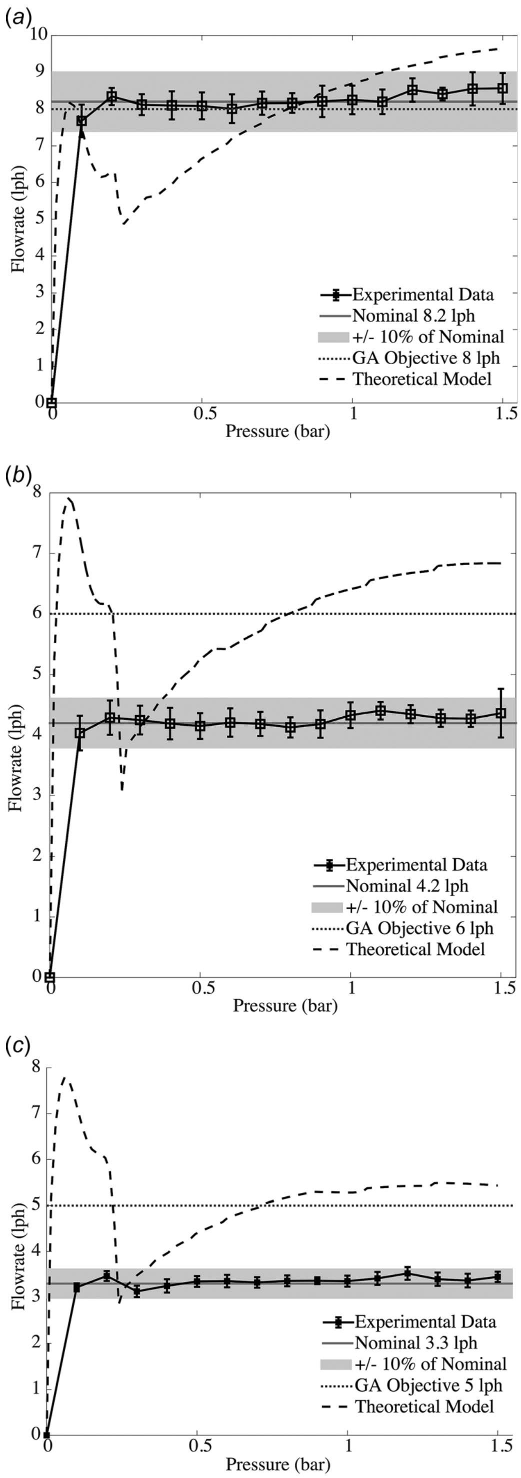

Fig. 3 Flow rate versus inlet pressure for emitters designed using the optimization process presented in this study. The three dripper designs with geometries presented in Table 1 are represented, optimized for 8 lph (*a*), 6 lph (*b*), and 5 lph (*c*) (horizontal dotted lines), with corresponding measured nominal flow rates of 8.2 lph, 4.2 lph, and 3.3 lph (horizontal gray lines), respectively. All emitters have an activation pressure of ≤0.2 bar. Two emitters for each specified flow rate were precision machined and tested. The gray band shows the ±10% allowed variation from nominal per industry standards. The black boxes with error bars denote the average and standard error of the 8 experimental data points collected per pressure reading. The dashed line represents the theoretical model prediction, which shows an accurate activation pressure.

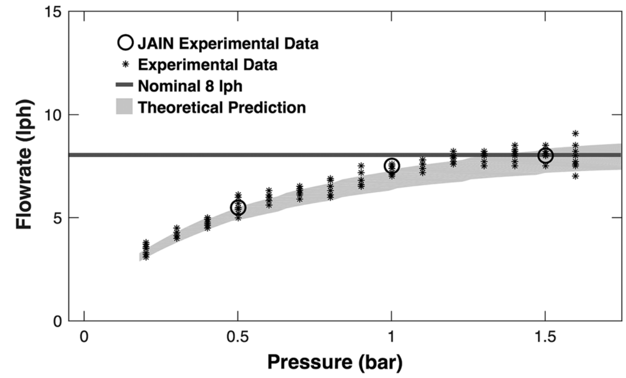

Fig. 4 Manufacturing error sensitivity for an 8 lph dripper produced by Jain Irrigation. This plot is adapted from Ref. [16], showing the variation in expected flow rate (gray band) over the same pressure range investigated in this study, due to tolerances of ±0.01 mm on D_{ch} and ±0.05 mm on W_{ch}. The gray line is the nominal flow rate specified by Jain, with the circles showing results from their data sheet. Experimental data were collected at MIT using the process described in Ref. [16].

should be refined to predict dripper behavior of varying flow rates beyond 8 lph with greater accuracy, Eq. (2) can be used with the optimization process presented in this study to design new dripper architectures and accurately predict their performance.

5 Validation Using Injection-Molded Prototypes

To validate the reduced MCIP in drip emitters manufactured using the same processes as existing commercial emitters, ten prototypes were manufactured by Jain Irrigation using the optimized geometry for the 8 lph dripper (Table 1). The drip emitters were made from polypropylene and were manufactured without significant added costs or changes to the injection molding processes by simply changing the mold insert that forms the internal flow features. This test confirmed our assumption that the optimal designs could be readily incorporated into existing manufacturing and distribution channels.

The average flow rate as a function of inlet pressure for the injection-molded prototype emitters was characterized by Jain Irrigation according to IS guidelines [22]. Figure 5 compares the measured performance of our prototypes (Massachusetts Institute of Technology (MIT)) to the published performance of commercially available 8 lph on-line PC drip emitters produced by Jain Irrigation [23], Toro [24], and Netafim [25]. The optimized injection-molded emitters show an activation pressure of 0.15±5 bar. This value is 21.4% the activation pressure of 0.70 bar for the Netafim emitter, and 16.7% the activation pressure of 0.90 bar for the Jain and Toro emitters. Our prototype emitter was able to maintain ±10% variation in its nominal flow rate (per industry standards) of 8.2 lph up to a pressure of 4 bar.

6 Cost Savings With Low Minimum Compensating Inlet Pressure Emitters

A detailed analysis of the capital cost of solar powered drip irrigation systems was conducted to assess the potential benefit of disseminating our PC drip emitters over currently available emitters in off-grid markets. As a benchmark, the capital cost of an off-grid, solar-powered drip irrigation system servicing a representative 1 acre (100 m × 40 m) banana farm was estimated using component costs from two different sources. The first source includes price lists from tier 1 drip irrigation companies [26,27], which is representative of global average costs based on a combined global market share of 35% [28]. The second price list is used by the Government of Gujarat (India) to be representative of India [6,29], which accounts for 118 million farm holdings [30]

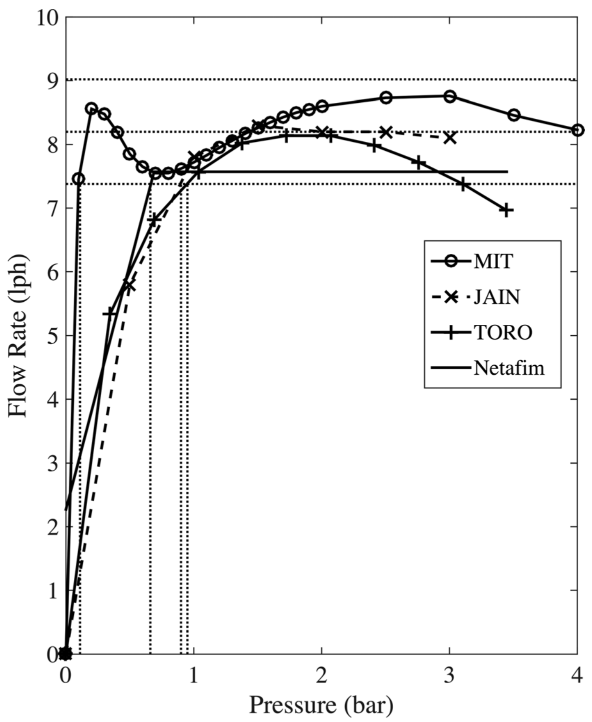

Fig. 5 Flow rate versus inlet pressure for the optimized emitter (MIT) compared to commercially available 8 lph emitters. The optimized emitter (MIT) is depicted as the bold line with circular markers and has an activation pressure that is 21.4% that of Netafim's [25] (bold black line) and 16.7% that of Toro's [24] (bold line with plus markers) and Jain's [23] (dashed line with cross markers). The results for the MIT emitter are averaged data from ten injection molded emitters; the coefficient of variation at every tested pressure point is less than 0.08. The data for the commercial emitters were obtained from their respective specification sheets. The vertical dotted lines denote activation pressures. The horizontal dotted lines denote ±10% variation from the MIT dripper's nominal flow rate of 8.2 lph, which corresponds to allowable industry standards.

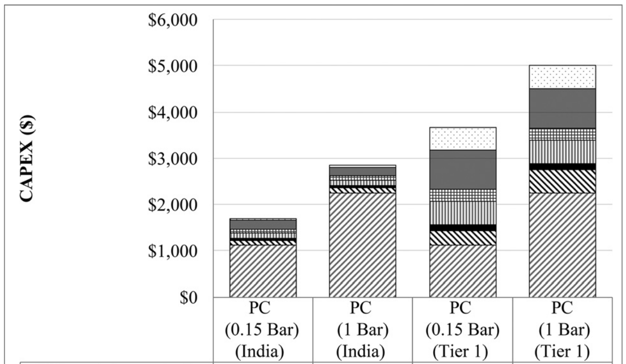

	PC (0.15 Bar) (India)	PC (1 Bar) (India)	PC (0.15 Bar) (Tier 1)	PC (1 Bar) (Tier 1)
□ Valves, joiner and other accessories	$46	$46	$500	$500
Filter (Sand+Disc)	$185	$185	$850	$850
Emitter (8 lph PC)	$86	$86	$260	$260
Lateral (16 mm)	$115	$115	$500	$500
■ Submain (63 mm)	$49	$49	$140	$140
Pump	$92	$115	$300	$500
Solar	$1,125	$2,250	$1,125	$2,250

Fig. 6 Capital cost analysis for a representative solar-powered, off-grid drip irrigation system in global markets (rated in $USD). Capital cost analysis of the drip irrigation system required for a representative 1 acre banana farm operating at (*a*) 1.55 bar (assuming 0.15 bar dripper activation pressure) and (*b*) 2.4 bar (assuming 1 bar dripper activation pressure) in both Indian and global (tier 1) markets. The estimated capital cost includes the smallest available solar pump required to move water from the source through a system of lateral pipes and drip emitters, sized for 1 day of autonomous off-grid use, a filter system to reduce emitter clogging, pipes to convey water from the source to the drip emitters, valves and joints, and 8 lph drip emitters to produce a controlled flow of water near the plant roots.

and 11.2% of the world's arable land [31]. The assumed banana crop spacing was 2 m × 2 m [6]. The water source was assumed to be surface water (water depth < 5 m, which is true for 63% of irrigated farms globally [15]). This type of water source is usually high in sand and biological matter, requiring a combination of a sand filter coupled with a disk filter.

The full drip system was designed based on best practices described in publically available resources [6,13,14]. The main components of the drip system included the smallest available solar pump required to move water from the source through a system of lateral pipes and drip emitters (accounting for the MCIP of the drip emitters, which were assumed to be either conventional or optimized based on Fig. 5), a filter system required to remove sediments from the water source to reduce emitter clogging, pipes to convey water from the source to the drip emitters, valves such as ball valves, flush valves, and backflow valves, drip emitters, and other pipe connectors and drip accessories. The full system contained 1000 8 lph on-line drip emitters, 2000 m of lateral polyethylene pipe, 100 m of submain PVC pipe, a sand and disk filter, and a pump (1 HP assuming a 0.15 bar MCIP for prototype drip emitters and 2 HP assuming 1 bar MCIP for conventional drip emitters based on Fig. 5). The solar power system was sized to provide 1 day of autonomy entirely off-grid in order to allow farmers to irrigate continuously and not be dependent on the intermittency of solar. The pump efficiency was assumed to be 40% (efficiency of commonly available pumps in this flow rate and pressure range) and the solar powering system cost was taken at $1.5/W (half the cost for the solar modules and the other half for nonmodular costs such as batteries, mounting structures, and wiring).

Figure 6 shows the cost breakdown of a solar-powered, 1 acre drip system using 8 lph drip emitters of the design shown in Fig. 1, with activation pressures of 1 bar (current technology) versus 0.15 bar (our optimized design). Drip emitters rated for 8 lph would be used on tree crops, such as bananas, dates, olives, or citrus. Figure 6 demonstrates how the overall capital cost of an off-grid surface water drip system could be reduced by more than 40% in India and 27% globally by simply lowering the activation pressure of the drip emitters without changing the laterals, submain lines, filter, or capital cost of the emitters.

7 Conclusions

This study presents the design and validation of a suite of on-line PC drip irrigation emitters with a substantially lower activation pressure than commercially available products. A genetic algorithm was used to optimize eight geometric parameters of PC drip emitters using a recently published fluid–structure interaction model of on-line PC drip emitter performance. To the authors' knowledge, this fluid–structure interaction model is the first to give a fully quantitative description of pressure-compensating behavior in drip emitters. While the model was able to parametrically describe the behavior of commercially available 8 lph drippers in our prior work, its prediction of the flow rate versus pressure relationship deviated significantly from experimental results for the three emitter designs presented in this study. Nevertheless, the model was able to accurately predict the low MCIP. Combined with a correction function presented herein that enables the accurate prediction of the anticipated nominal flow rate, the theory presented in this work can enable irrigation engineers to optimize drip emitter geometries for significantly lower MCIPs than those offered by commercial products.

This theory enabled the design innovation of an 8.2 lph PC drip emitter with an MCIP of 0.15 ± 0.05 bar, which is as low as 16.7% the activation pressure of current commercial products based on published performance data from manufacturers. Our optimization method was also used to design 3.3 and 4.2 lph drip emitters with MCIPs below 0.2 ± 0.05 bar. The performance of all three of these drippers was experimentally validated using a series of precision-machined prototypes. A limited production run of injection-molded prototypes of the 8.2 lph drippers was accomplished with minimal cost and modification to existing manufacturing equipment. Their performance matched that of the precision-machined prototypes, with an MCIP of 0.15 bar. The manufacturing constraints imposed by Jain Irrigation ensured that the new designs could be readily incorporated into existing manufacturing and distribution channels. A detailed analysis of the capital cost of fully off-grid solar powered drip irrigation systems confirmed that minimizing the MCIP of drip emitters could significantly reduce the capital cost of off-grid systems, by 27% globally and 40% in Indian markets.

Future work will include improving the fluid–structure interaction model by empirically deriving an expression for the orifice loss coefficient as a function of its geometry and size. Accuracy of the model may be further increased by accounting for additional losses in the fluid network, such as when the water must flow around the lands and into the channel (Fig. 1(*d*)), and accounting for manufacturing tolerances and their impact on flow behavior. Our future efforts will also involve expanding the fluid–structure interaction model to in-line PC drip emitter architectures and using a similar optimization method to minimize the MCIP for the in-line case. This work will include extensive clog testing of the new on-line and in-line drip emitter designs, and field tests to consider other possible performance tradeoffs that may result from operating drip irrigation systems at a lower inlet pressure.

Acknowledgment

The authors would like to thank Mr. Abhijit Joshi (Jain Irrigation Systems Ltd.) for his continued feedback on this research. The authors would also like to acknowledge Dan Dorsch for his support throughout the project. We thank Devarajan Ramanujan and Susan Amrose for their help editing this manuscript.

Funding Data

- Jain Irrigation Systems Ltd.
- Tata Center for Technology and Design at MIT.

References

[1] Iqbal, M., Sahi, F.-U.-H., Hussain, T., Aadal, N. K., Azeem, M. T., and Tariq, M., 2014, "Evaluation of Comparative Water Use Efficiency of Furrow and Drip Irrigation Systems for Off-Season Vegetables Under Plastic Tunnel," Int. J. Agric. Crop Sci., **7**(4), pp. 185–190.

[2] Namara, R. E., Upadhyay, B., and Nagar, R. K., 2005, "Adoption and Impacts of Microirrigation Technologies Empirical Results From Selected Localities of Maharashtra and Gujarat States of India," International Water Management Institute, Colombo, Sri Lanka, Technical Report No. 93.

[3] Nkya, K., Mbowe, A., and Makoi, J. H. J. R., 2015, "Low-Cost Irrigation Technology, in the Context of Sustainable Land Management and Adaptation to Climate Change in the Kilimanjaro Region," J. Environ. Earth Sci., **5**(7), pp. 45–56.

[4] Sivanappan, R. K., 1994, "Prospects of Micro-Irrigation in India," Irrig. Drain. Syst., **8**(1), pp. 49–58.

[5] Brouwer, C., Prins, K., Kays, W. M., and Heibloem, M., 1988, "Irrigation Water Management: Irrigation Methods," Training Manual No. 5, Food and Agriculture Organization, Rome, Italy.

[6] National Committee on Plasticulture Applications, 2017, "Horticulture, Ministry of Agriculture, Government of India, Microirrigation," Government of India, New Delhi, India.

[7] Irz, X., Lin, L., Thirtle, C., and Wiggins, S., 2001, "Agricultural Productivity Growth and Poverty Alleviation," Develop. Policy Rev., **19**(4), pp. 449–466.

[8] Tiffin, R., and Irz, X., 2006, "Is Agriculture the Engine of Growth?," Agric. Econ., **35**(1), pp. 79–89.

[9] Thirtle, C., Lin, L., and Piesse, J., 2003, "The Impact of Research-Led Agricultural Productivity Growth on Poverty Reduction in Africa, Asia and Latin America," World Develop., **31**(12), pp. 1959–1975.

[10] Cervantes-Godoy, D., and Dewbre, J., 2010, "Economic Importance of Agriculture for Poverty Reduction," OECD Food, Agriculture and Fisheries Papers, OECD Publishing, Paris, Paper No. 23.

[11] Shashidhara, K. K., Bheemappa, A., Hirevenkanagoudar, L. V., and Shashidhar, K. C., 2007, "Benefits and Constraints in Adoption of Drip Irrigation Among the Plantation Crop Growers," Karnataka J. Agric. Sci., **1**(20), pp. 82–84.

[12] Mahindra, 2017, "Design of EPC Drip Irrigation System," Mahindra, Mumbai, India, accessed Mar. 1, 2017, http://www.epcmahindra.com/pdf/how_to_arrive.pdf

[13] RainBird, 2000, "Low-Volume Landscape Irrigation Design Manual," Rain Bird Sales, Azusa, CA, accessed Mar. 1, 2017, http://www.rainbird.com/documents/drip/lowvolumeguide.pdf

[14] Hunter, 2012, "Drip Irrigation Design and Installation Guide," Hunter Industries, San Marcos, CA, accessed Mar. 1, 2017, https://www.hunterindustries.com/sites/default/files/dg_plddesign guide_dom.pdf

[15] Dubois, O., 2011, *The State of the World's Land and Water Resources for Food and Agriculture: Managing Systems at Risk*, Earthscan, London.

[16] Shamshery, P., Wang, R.-Q., Tran, D. V., and Amos, G., and Winter, V., 2017, "Modeling the Future of Irrigation: A Parametric Description of Pressure Compensating Drip Irrigation Emitter Performance," PloS One, **12**(4), p. e0175241.

[17] Shamshery, P., 2016, personal communication.

[18] Taylor, K., Shamshery, P., Wang, R., and Winter, A., 2015, "A Mathematical Model for Pressure Compensating Emitters," ASME Paper No. DETC2015-47519.

[19] Burt, C., and Feist, K., 2013, "Low-Pressure Testing: Microirrigation Emitters," Irrigation Training & Research Center (ITRC), San Luis Obispo, CA, Technical Report No. R 13-004.

[20] Boothroyd, G., 1994, *Product Design for Manufacture and Assembly*, Vol. 26, Elsevier, New York.

[21] Osswald, T. A., Turng, L.-S., and Gramann, P. J., 2008, *Injection Molding Handbook*, Carl Hanser Publishers, Cincinnati, OH.

[22] BIS, 1997, "Irrigation Equipment—Emitters—Specification," Bureau of Indian Standards, New Delhi, India, Standard No. IS 13487.

[23] JISL, 2015, "J-SC-PC-Plus: Technical Datasheet," Jain Irrigation Systems Ltd., Jagaon, India, accessed Feb. 17, 2017, http://jisl.co.in/pdf/catalogue_2015/drip/drippers/j_sc_pc_plus_emitter.pdf

[24] TORO, 2017, "Turbo-SC PC Emitter (T-DPJ08-A)," TORO Company, Riverside, CA, accessed Feb. 17, 2017, https://cdn.toro.com/en/~/media/files/toro/professional-contractor/landscape-drip/turbo-sc-plus/turbo-sc-ss.ashx

[25] Netafim, 2006, "WPC Online Non CNL Emitter," Netafim, Tel Aviv, Israel.

[26] Netafim, 2016, "General Price List," Netafim Ltd., Tel Aviv, Israel, accessed Mar. 1, 2017, http://www.netafim.com.ro/netafim-catalog-2016.pdf

[27] TORO, 2017, "Price List," TORO, Bloomington, MN, accessed Mar. 1, 2017, https://cdn.toro.com/en/~/media/files/toro/page/parts/alt002_pricelist_2017

[28] Markets and Markets, 2016, "Microirrigation Systems Market by Type (Drip and Microsprinkler), Application (Orchard Crops & Vineyards, Field Crops, and Plantation Crops), End-User (Farmers and Industrial Users), and by Region - Global Forecast to 2021," marketsandmarkets.com, accessed Mar. 1, 2017, https://www.marketsandmarkets.com/Market-Reports/micro-irrigation-system-market-566.html

[29] GGRC, 2016, "Pricelist of MIS Components," Gujarat Green Revolution Company Limited, Vadodara, India, accessed Dec. 12, 2016, http://ggrc.co.in/documents/PriceList_MIS_31_12_2015.pdf

[30] Agriculture Census, 2014, "Government of India—All India Report on Number and Area of Operational Holdings," Government of India, New Delhi, India, accessed Mar. 1, 2017, http://agcensus. nic.in/document/agcensus2010/completereport.pdf

[31] The Food and Agriculture Organization, The World Bank, and Arable Land (Hectares), 2017, "Arable Land (Hectares)," World Bank Group, Washington, DC, accessed Mar. 3, 2017, http://data.worldbank.org/indicator/ag.lnd.arbl.ha?end=2014start=1961view=chart